

Herschel-PACS observations of Nebulae Ejected by Massive Stars *

Chloi Vamvatira-Nakou¹, Pierre Royer², Damien Hutsemékers^{1,3}, Gregor Rauw¹,
Yaël Nazé^{1,3}, Katrina Exter², Christoffel Waelkens² and Martin Groenewegen⁴

¹ Institut d'Astrophysique et de Géophysique, Université de Liège, Belgium

² Instituut voor Sterrenkunde, Katholieke Universiteit Leuven, Belgium

³ FRS-FNRS, Belgium ⁴ Royal Observatory of Belgium

Abstract: The study of the nebulae ejected from Luminous Blue Variables and the circumstellar bubbles around Wolf-Rayet stars, which radiate strongly in the infrared due to the heating of dust, is crucial for the understanding of the massive stars evolution. With Herschel we are able to observe these objects in the far-infrared region. In the context of the Mass-loss from Evolved StarS guaranteed time key program, we obtained imaging and spectroscopic observations of nebulae associated with Luminous Blue Variable and Wolf-Rayet stars using PACS, one of the three instruments on-board Herschel. A description of these observations, data analysis and preliminary results are presented.

1 Introduction

LBV stars represent a short stage ($\sim 10^4 - 10^5$ yr) in the evolution of massive stars with initial mass $>40 M_{\odot}$. An early-type O star evolves into a WR star by losing a significant fraction of its initial mass. One way to lose mass is through stellar winds. In the last few years the mass-loss rates of O stars have been revised strongly downwards (Fullerton et al. 2006, Puls et al. 2008). This highlights the key role played by episodes of extreme mass-loss in an intermediate evolutionary phase (LBV or Red Supergiant phase). The main characteristics of these stars are photometric variability, from giant eruptions, ≥ 2 mag, to small oscillations, ~ 0.1 mag, high luminosity, $\sim 10^6 L_{\odot}$, and high mass-loss rate, $\sim 10^{-5} - 10^{-4} M_{\odot} \text{ yr}^{-1}$ (Humphreys & Davidson 1994). Most LBVs are surrounded by ejected nebulae (Hutsemékers 1994, Nota et al. 1995). Progressively, the outer layers of the star are removed revealing a bare core becoming a WR star which is a hot, luminous object with strong broad emission lines due to stellar winds. These winds have smaller mass-loss rates than LBV winds but higher velocities, up to 3000 km s^{-1} . They interact with the material ejected during the LBV phase, creating circumstellar bubbles observed around many WR stars. A significant fraction of the Galactic WR stars may be surrounded by nebulae (Marston 1997), but not all of them are ejecta nebulae.

There are many questions about the detailed evolution of these massive stars. We still do not know when and how these nebulae are formed, what causes the strong mass-loss phase to start and

*Herschel is an ESA space observatory with science instruments provided by European-led Principal Investigator consortia and with important participation from NASA.

what leads to the giant eruptions observed in some LBVs. Also, important quantities such as the nebular dust mass and the composition of the gas (CNO abundances) are very uncertain. Previous infrared studies of LBV nebulae have revealed that they contain dust and CO (McGregor et al. 1988, Hutsemékers 1997, Nota et al. 2002). With the ESA's Herschel Space Observatory (Pilbratt et al. 2010) we are able to study these nebulae in the far-infrared with high angular and spectral resolutions for the first time.

2 Our project with Herschel

As part of the Herschel Guaranteed Time Key Program entitled MESS - Mass-loss of Evolved StarS (Groenewegen et al. 2010, in preparation), we lead a project aiming at a detailed study of the gas and the dust in the circumstellar environments around LBVs and WR stars, so as to determine their properties. The accurate photometric maps of the far infrared emission provided by the instruments on-board Herschel will give us detailed information on the basic parameters of the dust shells. The combination of spectroscopic observations with optical data can provide accurate CNO abundances. Additionally, we can determine the properties of the neutral gas and of the photo-dissociation regions (PDR). Depending on the observed features, we will also be able to examine the dust mineralogy, estimate the mass and the location of the molecular gas and study the formation of dust in these nebulae. The list of our targets contains the LBVs AG Car, HR Car, WRA 15-751 and G79.29+0.46, the candidate LBVs He 3-519 and HD 168625 and the WR nebulae M 1-67 and NGC 6888. They will all be observed with the PACS photometer, while spectroscopic observations will be made for the brightest ones. In the following we present preliminary results for He 3-519 and WRA 15-751.

3 The LBV candidate He 3-519

He 3-519 is located in the Carina spiral arm of our Galaxy near some of the best known LBVs. Hoffleit (1953) discovered a shell nebula around it and Henize (1976) found that its spectrum was similar to that of AG Car. Stahl (1986, 1987) noted spectroscopic similarities to Ofpe/WN9 stars and published a [N II] λ 6584 CCD image of the nebula. Davidson et al. (1993) suggested that He 3-519 may be a post-LBV object and Smith et al. (1994) classified it as a WN 11 star, concluding that its nebula is a WR ring nebula.

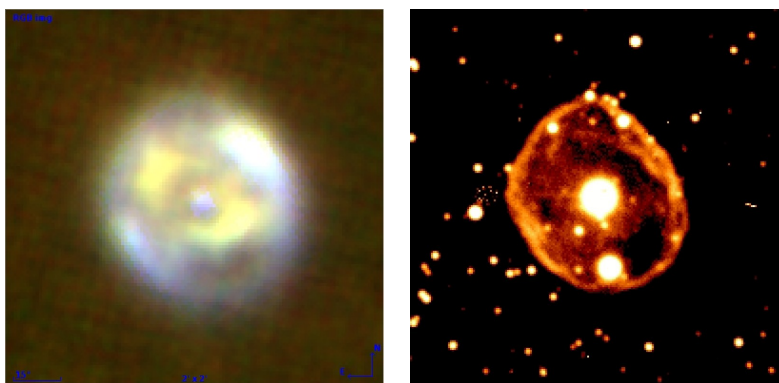


Figure 1: The nebulae around He 3-519. *Left*: morphology in the IR (RGB image with R being the PACS 100 μ m image, G the PACS 70 μ m image and B the Spitzer 24 μ m image). *Right*: H α image. The dimensions of both images are 2 \times 2 arcmin. North is up and East is to the left.

The photometric observations were carried out using the Photo Array Camera and Spectrometer (PACS, Poglitsch et al. 2010). The scan map observing mode was used. For each of the two ‘blue’ filters (70, 100 μm), two orthogonal scan maps were obtained, so that our final data set consists in maps at 70, 100 and 160 μm . The data reduction was performed using Herschel Interactive Processing Environment (HIPE, Ott 2010) and following the basic data reduction steps. Figure 1 shows an RGB image of the nebula around He 3-519, which is a combination of two PACS scan maps at 70 μm (G) and 100 μm (R) with a Spitzer image at 24 μm from the archive (B), together with the nebula in the optical region ($\text{H}\alpha$). In the $\text{H}\alpha$ image the nebula appears to be more elliptical with a thin shell structure, while the nebulae appears to have a more complicated structure in the infrared RGB image. Its diameter is approximately 80 arcsec in the IR images. In the $\text{H}\alpha$ image the nebula has a diameter of about 62 arcsec.

4 The LBV WRA 15-751

WRA 15-751 was identified as a galactic LBV by Hu et al. (1990). Hutsemékers & Van Drom (1991) found that it is surrounded by a ring nebula of ~ 22 arcsec in diameter. De Winter (1992) detected a cool dusty circumstellar shell around it with strong emission in the far-IR. Voors et al. (2000) derived many properties of the circumstellar dust around WRA 15-751 by modeling ground-based IR imaging around 10 μm and ISO spectroscopic observations: the dust shell is detached and slightly elongated, there is neutral gas outside the dust region and ionised gas only in the inner part of the dust region and the dust contains mostly large grains and a minor population of warm very small grains.

The PACS photometric observations were carried out in a similar way as those of He 3-519. For the spectroscopic observations, we used the SED observing template, providing a complete coverage between 52 and 220 μm . The PACS maps at 70 and 160 μm are shown in Figure 2, together with an $\text{H}\alpha$ image. In the PACS images, the nebula surrounding WRA 15-751 has clearly a ring shape with a diameter of about 40 arcsec. Its central part, with a diameter of about 10 arcsec, is fainter than the outer ring area. The central star is not visible at these wavelengths. In the $\text{H}\alpha$ image the morphology is different and the nebula diameter is about 25 arcsec.

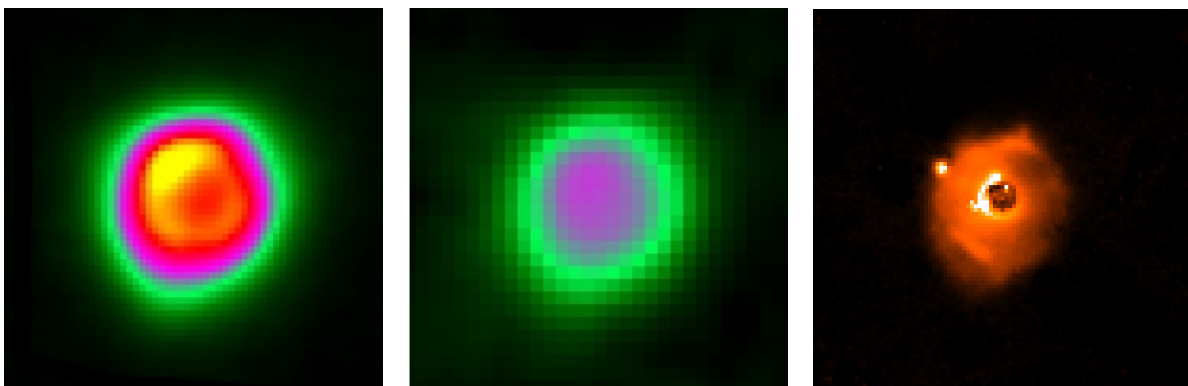


Figure 2: Images of WRA 15-751 obtained with PACS at 70 and 160 μm , together with an $\text{H}\alpha$ image of the nebula (from left to right). The dimensions are 1×1 arcmin for each image. North is up and East is to the left.

Aperture photometry was performed on the IR images, providing a good measurement of the nebular flux. We plotted the results along with IRAS data (from the IRAS point source catalogue) in Figure 3 and we fitted a modified black body described by a function of the form $B_{\nu} \lambda^{-\beta}$ (for a grain

emissivity $Q \sim \lambda^{-\beta}$). The best fit gives a temperature of 104.9 ± 2.4 K and an emissivity index of 1.4 ± 0.1 . This value is between amorphous carbon ($\beta = 1$) and silicates ($\beta = 2$). Voors et al. (2000) found an amorphous silicate emission feature and considered this as the main dust ingredient so as to model their spectrum, but finally they suggested also the presence of a small amount of very small carbon grains in order to explain a discrepancy of their model. Their model gave a temperature for small particles of 102 K at the inner and 82 K at the outer dust shell radius.

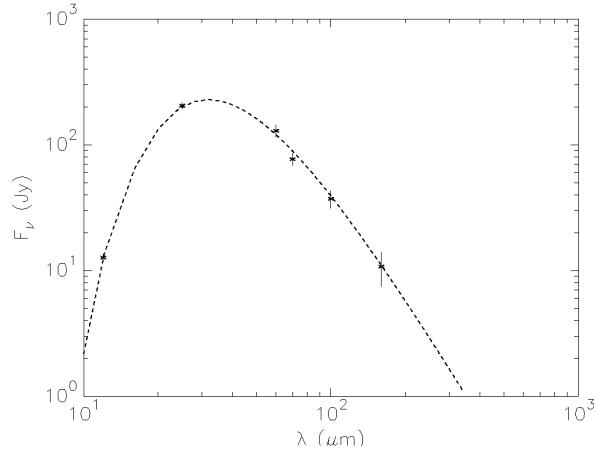


Figure 3: Modified black-body fit ($T = 104.9 \pm 2.4$ K and $\beta = 1.4 \pm 0.1$) to the derived fluxes from the PACS data of WRA 15-751 along with IRAS data.

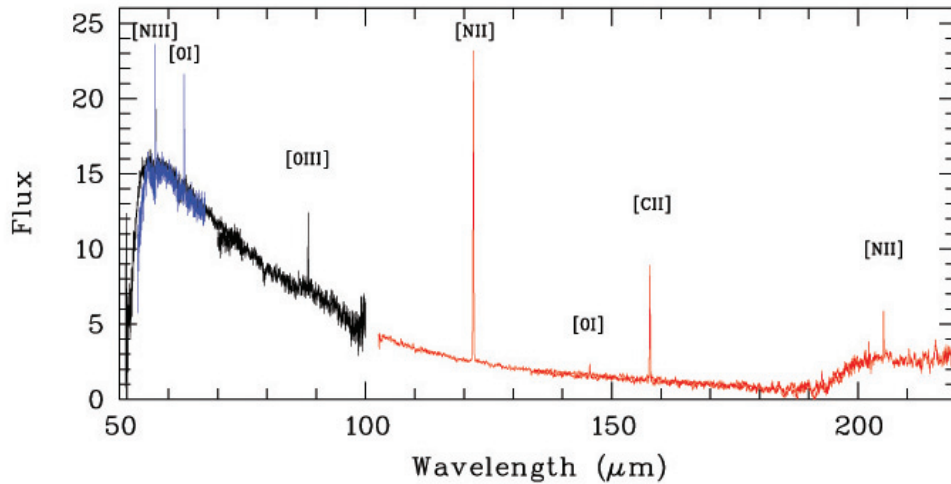


Figure 4: The PACS spectrum of WRA 15-751. Indicated are the lines [N III], [O I], [O III], [N II] and [C II]. The continuum shape below $55 \mu\text{m}$ results from a yet-imperfect spectral response function correction, while above $190 \mu\text{m}$ it results from a light leak, from the 2nd order ($70\text{-}100 \mu\text{m}$) to the 1st order ($>100 \mu\text{m}$).

The PACS spectrum is shown in Figure 4. The lines [N III] $\lambda 57.3 \mu\text{m}$, [O I] $\lambda 63 \mu\text{m}$ and $\lambda 145 \mu\text{m}$, [O III] $\lambda 88 \mu\text{m}$, [N II] $\lambda 122 \mu\text{m}$ and $\lambda 205 \mu\text{m}$ and [C II] $\lambda 158 \mu\text{m}$ are clearly visible with [N II] $\lambda 122 \mu\text{m}$ being the strongest one. The presence of these lines shows that gas around WRA 15-751 is highly ionised. The [O I] $\lambda 63 \mu\text{m}$ and [C II] $\lambda 158 \mu\text{m}$ fine-structure lines may indicate the presence of a PDR region. Such regions have already been detected in LBV nebulae (Umana et al. 2009, Umana et al. 2010). Voors et al. (2000), using ISO data, detected only the two lines [O III]

λ 88 μm and [N II] λ 122 μm , in the waveband 40-140 μm . Apart from these nebular lines and the dust continuum, no other features are detected. More details will be given in Vamvatira-Nakou et al. (2010, in prep.).

5 Conclusion and future work

Although the results presented here are very preliminary, it is clear that Herschel data with their high spectral and angular resolution give us unique information about the structure and the composition of the nebulae around evolved massive stars. Future work consists of analysing the photometric and spectroscopic Herschel data for each one of our targets and combining them with data taken in other spectral regions, so as to identify where exactly the dust is located with respect to the gas and to derive accurate measurements of dust and gas properties. By comparing the results found for our targets we aim at answering important questions about the origin of the nebulae and the evolution of massive stars in general.

Acknowledgements

PACS has been developed by a consortium of institutes led by MPE (Germany) and including UVIE (Austria); KU Leuven, CSL, IMEC (Belgium); CEA, LAM (France); MPIA (Germany); INAF-IFSI/OAA/OAP/OAT, LENS, SISSA (Italy); IAC (Spain). This development has been supported by the funding agencies BMVIT (Austria), ESA-PRODEX (Belgium), CEA/CNES (France), DLR (Germany), ASI/INAF (Italy), and CICYT/MCYT (Spain). CVN, PR, DH, GR, YN and KE acknowledge support from the Belgian Federal Science Policy Office via the PRODEX Programme of ESA. The Liège team acknowledges also support from the FRS-FNRS (Comm. Franç. de Belgique).

References

- Davidson K., Humphreys R.M., Hajian A. & Terzian Y., 1993, *ApJ*, 411, 336
Fullerton A.W., Massa D.L. & Prinja R.K., 2006, *ApJ*, 637, 1025
Henize K.G., 1976, *ApJS*, 30, 491
Hoffleit D., 1953, *Ann. Harvard Coll. Obs.*, 119, 37
Hu J.Y., de Winter D., Thé P.S. & Pérez M.R., 1990, *A&A*, 227, 17
Humphreys R.M. & Davidson K., 1994, *PASP*, 106, 1025
Hutsemékers D., 1994, *A&A*, 28, 81
Hutsemékers D., 1997, *ASPC*, 120, 316
Hutsemékers D. & Van Drom E., 1991, *A&A*, 251, 620
Marston A.P., 1997, *ApJ*, 475, 188
McGregor P.J., Hyland A.R. & Hillier D.J., 1988, *ApJ*, 324, 1071
Nota A., Livio M., Clampin M. & Schulte-Ladbeck R., 1995, *ApJ*, 448, 788
Nota A., Pasquali A., Marston A.P., Lamers H.J.G.L.M., Clampin M. & Schulte-Ladbeck R., 2002, *AJ*, 124, 2920
Ott, S. 2010, in press, arXiv1011.1209
Pilbratt G.L. et al. 2010, *A&A*, 518, L1
Poglitsch A. et al. 2010, *A&A*, 518, L2
Puls J., Markova N. & Scuderi S. 2008, *ASPC*, 388, 101
Smith L.J., Crowther P.A. & Prinja R.K., 1994, *A&A*, 281, 833
Stahl O., 1986, *A&A*, 164, 321
Stahl O., 1987, *A&A*, 182, 229
Umana G., Buemi C.S., Triglio C., Hora J.L., Fazio G.G. & Leto P., 2009, *ApJ*, 694, 697
Umana G., Buemi C.S., Triglio C., Leto P. & Hora J.L., 2010, *ApJ*, 718, 1036
Voors R.M.H. et al., 2000, *A&A*, 356, 501
De Winter D., Pérez M.R., Hu J.Y. & Thé P.S., 1992, *A&A*, 257, 632